

Article

Nonlinear Stochastic Adaptive Control for DFIG-Based Wind Generation System

Jian Zhang, Yong Wan *, Quan Ouyang  and Meng Dong

College of Automation Engineering, Nanjing University of Aeronautics and Astronautics, Nanjing 211106, China; alanzj@nuaa.edu.cn (J.Z.); ouyangquan@nuaa.edu.cn (Q.O.); dongmeng@nuaa.edu.cn (M.D.)

* Correspondence: wanyong@nuaa.edu.cn or wanyong17007@163.com

Abstract: The aim of this paper is to extract the maximum power from wind energy for the doubly fed induction generator based wind turbine system (DFIG-WT) under the continuous stochastic perturbations of wind speed. The DFIG-WT is modeled as the Itô stochastic differential equations. The stochastic backstepping control method and the gain suppressing inequality technique are employed to guarantee that the relative rotor speed to the optimal value is bounded in probability. Furthermore, we extend the bounded result to the asymptotic stability of the rotor speed control loop. In addition, the parametric uncertainties in DFIG-WT are also considered in our control synthesis. The simplicity, robustness and efficiency of the designed controller are verified under the special wind speed with white noise by the numerical simulation of a 660 KW DFIG-WT.

Keywords: DFIG; wind turbine; stochastic differential equations; stochastic backstepping control; stochastic wind speed; MPPT



Citation: Zhang, J.; Wan, Y.; Ouyang, Q.; Dong, M. Nonlinear Stochastic Adaptive Control for DFIG-Based Wind Generation System. *Energies* **2023**, *16*, 5654. <https://doi.org/10.3390/en16155654>

Academic Editor: Davide Astolfi

Received: 27 June 2023

Revised: 20 July 2023

Accepted: 25 July 2023

Published: 27 July 2023



Copyright: © 2023 by the authors. Licensee MDPI, Basel, Switzerland. This article is an open access article distributed under the terms and conditions of the Creative Commons Attribution (CC BY) license (<https://creativecommons.org/licenses/by/4.0/>).

1. Introduction

Energy is a critical factor in industrial growth; however, its development has led to increased greenhouse gas emissions and the production of hazardous and radioactive waste. As a result, the reserve of petroleum, a major energy source, is continuously decreasing, and energy demand will soon exceed supply. Nuclear energy, another significant source for industrial development, is not available to all countries due to expensive installation and political reasons, and it poses ecological risks. Therefore, the industrial sector must shift towards renewable energy sources for several reasons. One of the main advantages of renewable energy sources is that they do not emit greenhouse gases and do not produce toxic or radioactive waste.

Among these energy sources, wind energy is one of the fastest growing ones for electricity production worldwide, and DFIG-WT has become a popular wind power generation system due to its high energy conversion efficiency from variable speed operation and relatively low cost of power electronic converter. The performance of the DFIG-WT depends on the control systems applied on both the turbine and generator sides, which are typically designed using a cascade structure that includes a fast inner loop for power control of the doubly fed induction generator (DFIG) and a slow outer loop for speed control of the drivetrain. Below the rated wind speed, the critical control task is to maximize the captured wind energy through variable speed operation. This requires the DFIG-WT to be fully controllable and operated at an optimal rotor speed according to the stochastic wind speed.

Over the past decade, there has been extensive research on the modeling and control of DFIG-WT. This system has strong nonlinearities due to the aerodynamics of wind turbines, the coupled dynamics of the DFIG and wide operation in the stochastic wind speed. Direct power control (DPC) of DFIG-WT systems has been proposed in [1,2] and developed in [3,4]. An adaptive compensation control with quasi-synchronous rectification algorithm is first proposed to track maximum power in [5]. Furthermore, in [6], Xiong, LY

proposes a novel sliding mode control technique for DFIGs based on the fast exponential reaching law to track active/reactive power. Model predictive control is developed for the rotor-side converter (RSC) in [7]. Predictive rotor current control is developed under unbalanced and distorted grid conditions in [8] to control the output active/reactive power robustly. Fariba Fateh [9] utilizes feedback linearization to assume that the power capture coefficient and the desired rotor speed are instantaneously identified for tracking maximum power. However, all the above articles study deterministic systems. Several researchers study stochastic systems in which DFIG-WT is affected by the stochastic wind, such as in reference [10], who combine the conventional optimal torque control algorithm with the Fokker–Planck–Kolmogorov equation solved by the linear least square method to make the PDF shape of the rotor speed track the desired PDF shape as accurately as possible. Additionally, the work in [11] presents a new stochastic predictive control approach for variable-speed wind turbines to capture maximum power under the rated wind speed.

In the literature, several works have focused on the wind control problem using backstepping control. For example, backstepping-based direct power control is used to regulate output power under harmonic grid voltage in [12]. In addition, reference [13] proposes enhanced low-voltage ride through nonlinear backstepping control of DFIG-based wind turbines in stiff grid conditions. Moreover, Mechter [14] designs a backstepping controller in the presence of uncertainty based on fuzzy logic theory to extract optimal power for low wind speed. Furthermore, reference [15] develops an adaptive backstepping approach in DFIG-WT for nonlinear robust control of active and reactive power and utilizes FPGA to implement the effectiveness and the benefit of the proposed controller. However, the backstepping method in stochastic systems for asymptotic control is not investigated in DFIG-WT. On one hand, it is difficult to implement backstepping from deterministic systems to stochastic systems for their second-order differential term in the Itô formula, and the inequality technique is indispensable to avoid the control singularity. On the other hand, nonzero constants are definitively introduced into the Lyapunov analysis, while most of the literature can only achieve the boundness of state in probability. Reference [16] develops a novel gain suppressing inequality technique to realize the boundness in probability of involved signals and utilizes fuzzy logic to assure asymptotically stability in probability.

All the papers mentioned above and many others in the literature have not discussed the tracking of the maximum output power by tip slip ratio method in nonlinear stochastic backstepping control with the impact of parameter variations of DFIG-WT. This paper proposes adaptive nonlinear stochastic backstepping control based on the gain suppressing theorem of wind turbines for maximum power point tracking (MPPT).

The remainder of this paper is organized as follows. In Section 2, the Itô stochastic differential equation model of DFIG-WT is constructed; meanwhile, the problem formulation is stated. The preliminaries needed in this paper are stated in Section 3. The equivalent model and nonlinear stochastic backstepping control of DFIG are designed in Section 4 to asymptotically track the maximum output power, and stability proof is presented. A simulation study is carried out in Section 5 to validate the robustness of the proposed controller. Finally, the conclusion is provided in Section 6.

2. DFIG-Based Wind Generation System Modeling and Problem Formulations

The schematic diagram of the DFIG-based wind generation system is shown in Figure 1. The whole system has two main components: (i) The wind turbine contains the drivetrain system and the gearbox. (ii) The DFIG is directly connected to the alternating current (AC) grid by the stator, while the rotor is fed through a four-quadrant AC-to-AC converter.

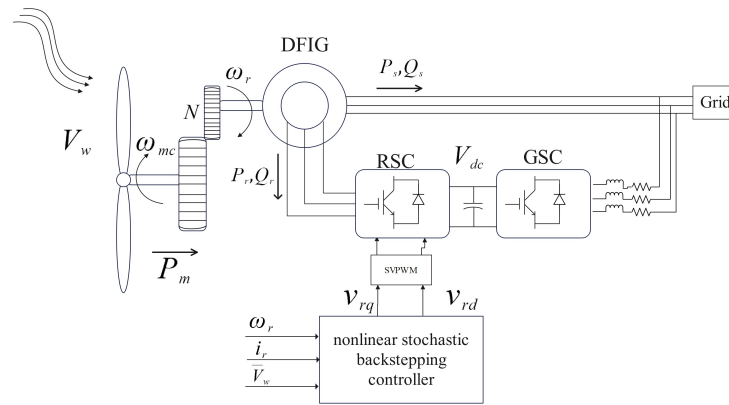


Figure 1. Schematic diagram of a DFIG-based wind generation system.

2.1. DFIG Model

In general, it is acceptable to employ the DFIG model defined in the dq frame with fixed stator flux for the transient stability analysis [17]. Furthermore, the dynamical equations with the electromagnetic torque expression are presented as follows [18]:

$$\frac{di_{rd}}{dt} = -\frac{R_r}{\sigma}i_{rd} + (\omega_0 - \omega_r)i_{rq} + \frac{u_{rd}}{\sigma}, \tag{1}$$

$$\frac{di_{rq}}{dt} = -\frac{R_r}{\sigma}i_{rq} - (\omega_0 - \omega_r)i_{rd} + \frac{u_{rq}}{\sigma} - \frac{(\omega_0 - \omega_r)V_s L_m}{\sigma \omega_0 L_s}, \tag{2}$$

$$T_e = -\frac{L_m V_s}{L_s \omega_0}i_{rq}, P_s = -\frac{3L_m}{2L_s}V_s i_{rq}, Q_s = -\frac{3L_m}{2L_s}V_s i_{rd} + \frac{3V_s^2}{2L_s \omega_0}, \tag{3}$$

where the rotor currents, i_{qr} and i_{dr} , are controlled by the rotor-side converter u_{rd} , u_{rq} . Constant $\sigma = L_r - L_m^2/L_s$, R_r is rotor resistance and ω_r is rotor speed.

Remark 1. In the above model, the AC bus frequency ω_0 and voltage V_s are considered to be constant [9], the q-axis is aligned with the stator flux and the stator resistance is neglected.

2.2. Wind Turbine Model

The mechanical motion equation for the wind turbine connected with the DFIG is described as [19]

$$\frac{d\omega_r}{dt} = \frac{Nn_p}{J}(T_m - T_e), \tag{4}$$

where N is the gearbox ratio defined as the ratio between the rotational speeds of the low-speed shaft ω_{mc} and high-speed shaft ω_r , n_p is the number of poles, J is the equivalent lumped mass moment of inertia of the blades, rotor shaft and drivetrain, and T_e is the electrical torque provided by the generator. Hence, one can obtain the relationship $\omega_r = Nn_p\omega_{mc}$.

Next, the aerodynamic power P_m captured by the wind turbine is given by

$$P_m = \frac{1}{2}\pi R^2 \rho C_p(\lambda, \beta)V_w^3, \tag{5}$$

where R is the blade radius in meter, ρ is the air density, V_w is wind speed and C_p is the power coefficient. C_p depends on the tip speed ratio λ and the pitch angle β . In this paper, we consider that the wind turbine operates in the subrated speed range; thus, β is set to be constant, i.e., $\beta = 0$. Further, the tip speed ratio λ satisfies

$$\lambda = \frac{R\omega_{mc}}{V_w}. \tag{6}$$

Based on (5) and (6), we obtain the mechanical torque expression as

$$T_m = \frac{P_m}{\omega_{mc}} = \frac{\pi R^3 \rho C_p}{2 \lambda} V_w^2 = \frac{\pi R^3 \rho}{2} C_q V_w^2, \tag{7}$$

where C_q is given by

$$C_q(\lambda) = \frac{0.44}{\lambda} \left[130 \left(\frac{1}{\lambda} - 0.0312 \right) - 5 \right] e^{-21 \left(\frac{1}{\lambda} - 0.8 \right)}. \tag{8}$$

Further, the C_q - λ characteristic is described in Figure 2. This figure indicates that there is one specific λ on which the wind turbine operates most efficiently, and C_q is the maximum. Generally, a variable-speed wind turbine imposes the $C_q^{max} = 0.0507$ to capture the maximum torque by varying the rotor speed to keep the system operating on optimal tip speed ratio $\lambda_{opt} = 7.19$.

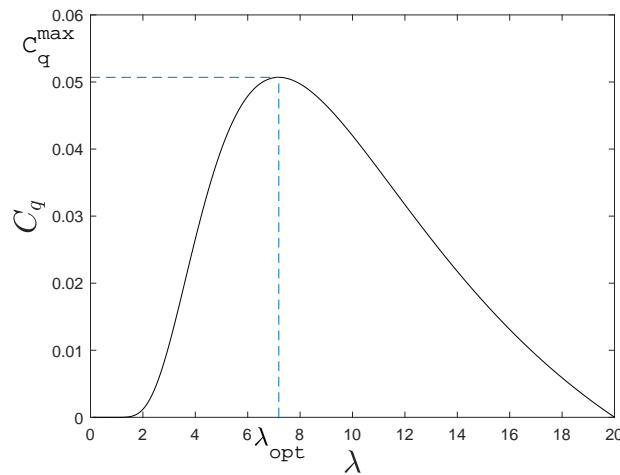


Figure 2. Curve of C_q - λ .

Subsequently, the desired optimal rotor speed ω_r^* can be calculated using (6) in the sense of λ_{opt} :

$$\omega_r^* = \frac{N n_p \lambda_{opt} \bar{V}_w}{R}, \tag{9}$$

and our control objective is to regulate the rotor speed ω_r to the optimal value ω_r^* to extract the maximum wind power.

Remark 2. Since it is difficult to measure the actual wind speed accurately, and there exists the shock phenomenon of the input mechanical torque of the wind turbine when the wind speed changes rapidly, we utilize the mean wind speed, i.e., \bar{V}_w , to replace the actual one in (9).

Equivalent Itô Form of (4)

According to (6)–(8), we find that the mechanical torque T_m is a nonlinear function of ω_r and V_w . Thus, for a specific wind speed such as $V_w = 15$ m/s, one can utilize the following second-order polynomial to approximate the T_m - ω_r mapping in the subrated speed range:

$$\bar{T}_m(\omega_r) = a\omega_r^2 + b\omega_r + c, \tag{10}$$

where $a = -0.02372$, $b = 2.104$, $c = -50.61$; see Figure 3 for the fitting performance.

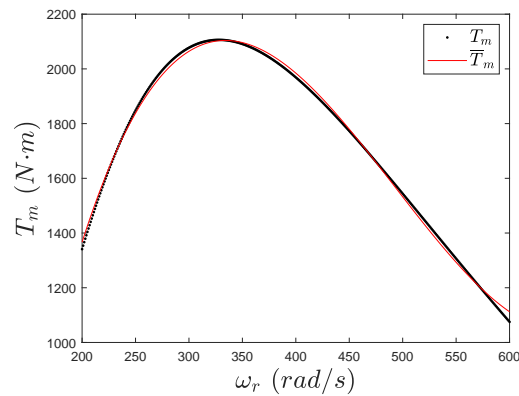


Figure 3. Fitting of T_m in the subrated speed range.

As depicted in [20,21], one can equivalently transform the mechanical torque shown in (7) into the following form:

$$T_m(\omega_r, V_w) = \bar{T}_m(\omega_r) + \Delta T_m, \tag{11}$$

where \bar{T}_m represents the torque with low fluctuations, and it is obtained by supposing that the wind speed equals its mean value \bar{V}_w , the term ΔT_m models the fitting error in Figure 3 and the influences of the stochastic fluctuations of wind speed that vary around its mean value, namely ΔV_w , which is often modeled by white noise [22]. Furthermore, this mechanical torque uncertainty is described as

$$\Delta T_m = k_0 h(\omega_r - \omega_r^*) W(t), \tag{12}$$

in which $h(\omega_r - \omega_r^*)$ represents the noise intensity function of the rotor speed, and it is thrice differentiable and passes through the origin, k_0 is gain of the function $h(\omega_r - \omega_r^*)$, and $W(t)$ is the white noise whose correlation function is $E[W(t)W(t + \tau)] = 2\pi K\delta(\tau)$, with K as the intensity of the white noise.

Based on (3) and (10)–(12), the wind turbine dynamical Equation (4) is equivalently transformed into the following form:

$$\frac{d\omega_r}{dt} = \frac{Nn_p}{J} \left(a\omega_r^2 + b\omega_r + c + \frac{L_m V_s}{L_s \omega_s} i_{rq} \right) + \frac{Nn_p}{J} k_0 h(\omega_r - \omega_r^*) W(t). \tag{13}$$

By applying the Itô differential law and considering the relationship between white noise and the wiener process [23], wind turbine system (13) is further transformed into the Itô stochastic differential equation as follows:

$$d\omega_r = \left[\frac{Nn_p}{J} \left(a\omega_r^2 + b\omega_r + c + \frac{L_m V_s}{L_s \omega_s} i_{rq} \right) + \left(\frac{Nn_p}{J} \right)^2 \pi K k_0^2 h(\omega_r - \omega_r^*) \frac{\partial h(\omega_r - \omega_r^*)}{\partial \omega_r} \right] dt + \frac{Nn_p}{J} \sqrt{2\pi K} k_0 h(\omega_r - \omega_r^*) dB, \tag{14}$$

where B is a wiener process.

As such, the overall DFIG-based wind generation system model is represented by (1), (2) and (14).

2.3. Problem Statement

Generally, the values of the DFIG generator parameter such as the rotor resistance, the rotor inductance, the stator inductance and the mutual inductance can not be acquired explicitly, because these parameters are not always constant under various complex operating conditions, and also, there exist relative measurement errors in the parametric identification process. Meanwhile, although the fitting error shown in Figure 3 is small and has been

modeled in (12), it is appropriate to consider the parameters a, b, c in (10) as the unknown ones, because the mean value \bar{V}_w , which is used to identify the values of a, b, c , reflects the trend of the wind speed and may vary slowly with respect to the timescale of transient stability analysis. Hence, seven parameters $a, b, c, R_r, L_s, L_r, L_m$ are viewed as unknown constants in this paper.

Furthermore, due to the inherent characteristic of the randomness of the wind speed, there exists a certain shock phenomenon for the input mechanical torque of the wind turbine, which is modeled as the wiener process in (14). As shown in Figure 4, in order to extract the maximum energy constantly from the stochastic wind that causes the DFIG rotor speed responses in the region of the MPPT above the startup speed ω_{rB} and below the rated value ω_{rC} , it is significant and challenging work to design the nonlinear stochastic adaptive control strategy for the DFIG to impose the rotor speed to rotate at the optimal rotor speed ω_r^* to maintain the MPPT condition C_q^{max} based on the Itô stochastic differential equation model (1), (2) and (14).

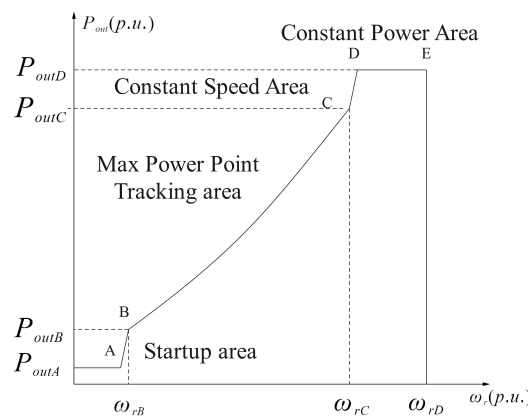


Figure 4. Relationship between the DFIG rotor speed and the output power.

3. Mathematic Preliminary

Consider the following stochastic nonlinear system:

$$dx = \mathbf{F}(x)dt + \mathbf{H}(x)dB, \tag{15}$$

where $\mathbf{x} \in \mathbb{R}^n$ is the state vector, \mathbf{B} is a q -dimensional independent standard wiener process in a complete probability space $(\Omega, \mathcal{F}_{t \geq 0}, P)$, $\mathbf{F} : \mathbb{R}^n \rightarrow \mathbb{R}^n$, and $\mathbf{H} : \mathbb{R}^n \rightarrow \mathbb{R}^{n \times q}$ are locally Lipschitz and satisfy $\mathbf{F}(0) = 0, \mathbf{H}(0) = 0$ for all $t \geq 0$. For a Lyapunov function $V \in C^2$, let $\mathcal{L}V$ denote the differential operator of V with respect to (15):

$$\mathcal{L}V = \sum_{j=1}^n \frac{\partial V}{\partial x_j} f_j(\mathbf{x}) + \frac{1}{2} \sum_{j,k=1}^n \sum_{l=1}^q \left\{ \frac{\partial^2 V}{\partial x_j \partial x_k} h_{jl}(\mathbf{x}) h_{kl}(\mathbf{x}) \right\}, \tag{16}$$

where h_{jl} represents (j, l) -element in the matrix $\mathbf{H}(\mathbf{x})$; f_j and x_j , respectively, represent the j th-element in the vectors $\mathbf{F}(\mathbf{x})$ and \mathbf{x} .

Remark 3. The form of $\mathcal{L}V$ is different from that in determination system for its second-order differential term $\frac{1}{2} \sum_{j,k=1}^n \sum_{l=1}^q \left\{ \frac{\partial^2 V}{\partial x_j \partial x_k} h_{jl}(\mathbf{x}) h_{kl}(\mathbf{x}) \right\}$ in the Itô formula. The Itô differential equation is a classic form of a stochastic nonlinear system, into which we transform the model of DFIG-WT for inherent stochastic wind speed in (14). Meanwhile, we introduce a second-order differential term that it is hard to design a controller by Lyapunov stable method. Hence, we utilize inequality techniques (19) and (20) to simplify the form of $\mathcal{L}V$ and process of design of stochastic backstepping controller; then, Lemma 1 is integrated with each step of the backstepping-based adaptive control design process to obtain the result that the output active/reactive power of DFIG-WT is bounded in

probability. Furthermore, employing Lemma 3 to achieve the asymptotical convergence of the output active/reactive power of DFIG-WT.

Lemma 1. Let ϱ be a positive constant, χ be a bounded and positive variable and b_j be an unknown but bounded positive constant. If the following inequality holds over $[0, t_W)$, then the involved signals $Z(t)$ and $v_j(t)$ are bounded in probability.

$$\mathcal{L}Z(t) \leq -\varrho Z(t) - \sum_{j=1}^n (b_j \mathcal{I}_{st}(v_j(t)) - 1) \dot{v}_j(t) + \chi, \tag{17}$$

where $Z(t)$ is a smooth positive definite function for $[0, t_W)$, and $v_j(t)$ is defined as a smooth function with $v_j(0)$ being bounded for $j = 1, 2, \dots, n$. $\mathcal{I}_{st}(v_j)$ is defined by

$$\mathcal{I}_{st}(v_j) = \left(e^{\frac{1}{2}v_j^2} v_j^2 + 2e^{\frac{1}{2}v_j^2} \right) \sin(v_j). \tag{18}$$

See the detailed proof in [16].

Lemma 2. Let p, q be positive real numbers satisfying $\frac{1}{p} + \frac{1}{q} = 1$. Then, if a, b are non-negative real numbers, $ab \leq \frac{a^p}{p} + \frac{b^q}{q}$ and equality holds if, and only if, $a^p = b^q$ [24].

Some important inequalities are inferred from Lemma 2 to simplify the form of $\mathcal{L}V$ as follows:

let $a = x^2y^2, b = \gamma^2, p = q = 2$ and $\gamma > 0$, then we have

$$x^2y^2 \leq \frac{1}{2}\gamma^{-2}x^4y^4 + \frac{1}{2}\gamma^2. \tag{19}$$

Further, let $a = x^3, b = y, p = \frac{4}{3}, q = 4$, then one obtains

$$x^3y \leq \frac{3}{4}x^4 + \frac{1}{4}y^4. \tag{20}$$

Furthermore, stochastic Barbalat’s lemma is employed to achieve the asymptotical convergence of the output active/reactive power of DFIG-WT.

Lemma 3. If the solution process $x(t)$ of system (15) is strongly bounded in probability, and

$$E \int_0^\infty |\beta(x(t))| dt < \infty, \tag{21}$$

where $\beta(\cdot)$ is a continuous function, then

$$\lim_{t \rightarrow \infty} \beta(x(t)) = 0, \text{ a.s. (almost surely)}. \tag{22}$$

See the detailed proof in [25].

4. Controller Design for DFIG-WT

To command the nonlinear systems (1), (2) and (14) and employ the Lyapunov stable method, the transformation around the operating point must be used to conceive the controller. The objective of RSC is to maintain the i_{rd} of the DFIG and the rotor speed ω_r of the wind turbine at the desired references. From the nonlinear system of DFIG-WT, to control i_{rd} and ω_r , we can adjust i_{rd} and i_{rq} by u_{rd} and u_{rd} , respectively. To achieve this task, in previous research, backstepping control is used. In this research, a new backstepping controller applied in a nonlinear stochastic system for rotor speed is proposed. We decompose the whole nonlinear control problem into some smaller ones. The conception

of stochastic backstepping control law is divided into various design steps. In each step, we calculate a virtual command from the tracking error, which will be used in the next step as a reference. We repeat the operation until obtaining the controller that will be applied to the system. It must be ensured, in each step, that the derivate of the Lyapunov function (definite positive) is always negative.

Firstly, we need a lot of variable substitution and to transform the DFIG-WT system around reference values of system state $\omega_r^*, i_{rd}^*, i_{rq}^*$. Let the right of (1), (2) and (14) equal zero; them, $\omega_r^*, i_{rd}^*, i_{rq}^*$ can be calculated. Define the error variables between the state, input and their reference value as $x_1 = \omega_r - \omega_r^*, x_2 = i_{rq} - i_{rq}^*, x_3 = i_{rd} - i_{rd}^*, u_1 = u_{rq} - u_{rq}^*, u_2 = u_{rd} - u_{rd}^*$, and denote $\theta_1 = -Nn_p a / J, \theta_2 = -2aNn_p \omega_r^* / J, \theta_3 = Nn_p b / J, \theta_4 = Nn_p L_m V_s / (JL_s \omega_s), \theta_5 = R_r / \sigma, \theta_6 = V_s L_m / (\omega_s \sigma L_s), \theta_7 = 1 / \sigma, c_1 = \omega_s - \omega_r^*, c_2 = i_{rq}^*, c_3 = i_{rd}^*, c_4 = Nn_p k_0 \sqrt{\pi K} / J$.

Thus, (1), (2) and (14) can be represented by the equivalent form:

$$\begin{aligned} dx_1 &= \left(-\theta_1 x_1^2 - \theta_2 x_1 + \theta_3 x_1 + c_4^2 h(x_1) \frac{\partial h(x_1)}{\partial x_1} + \theta_4 x_2 \right) dt + \sqrt{2} c_4 h(x_1) dB, \\ dx_2 &= (-\theta_5 x_2 + \theta_6 x_1 + c_3 x_1 + (x_1 - c_1) x_3 + \theta_7 u_1) dt, \\ dx_3 &= (-\theta_5 x_3 - c_2 x_1 + c_1 x_2 - x_1 x_2 + \theta_7 u_2) dt. \end{aligned} \quad (23)$$

To facilitate the analysis, the changes in coordinates are proposed as $e_1 = x_1, e_2 = x_2 - x_2^*$, and $e_3 = x_3$. The designed function x_2^* is virtual control unit.

Step 1 : For the first subsystem of system (23), choose the stochastic Lyapunov function $V_1 = \frac{1}{4} e_1^4$. The differential operator of V_1 according to (16) is

$$\mathcal{L}V_1 = e_1^3 \left(-\theta_1 x_1^2 - \theta_2 x_1 + \theta_3 x_1 + c_4^2 h(x_1) \frac{\partial h(x_1)}{\partial x_1} + \theta_4 (e_2 + x_2^*) \right) + 3c_4^2 e_1^2 h^2(x_1). \quad (24)$$

In the stochastic system, e_1 is a stochastic process for the external wiener process dw , and V_1 is considered as the function of the stochastic process. Utilizing the property of Lemma 2, four terms in (24) can be further changed into

$$\begin{aligned} -\theta_1 e_1^3 x_2^2 &\leq \theta_1 \frac{1}{2\lambda_1^2} e_1^6 x_1^4 + \theta_1 \frac{1}{2} \lambda_1^2, \\ c_4^2 e_1^3 h(x_1) \frac{\partial h(x_1)}{\partial x_1} &\leq c_4^2 \frac{1}{2\lambda_2^2} e_1^6 \left(h(x_1) \frac{\partial h(x_1)}{\partial x_1} \right)^2 + c_4^2 \frac{1}{2} \lambda_2^2, \\ \theta_4 e_1^3 e_2 &\leq \theta_4 \frac{3}{4} e_1^4 + \theta_4 \frac{1}{4} e_2^4, \\ 3c_4^2 e_1^2 h^2(x_1) &\leq 3c_4^2 \frac{1}{2\lambda_3^2} e_1^4 h^4(x_1) + 3c_4^2 \frac{1}{2} \lambda_3^2, \end{aligned} \quad (25)$$

where the designed constants $\lambda_1, \lambda_2, \lambda_3$ are positive.

On the basis of (25), one can transform (24) into the following inequality

$$\mathcal{L}V_1 \leq -\theta_2 e_1^4 + e_1^3 (W_1 + \theta_4 x_2^*) + \theta_4 \frac{1}{4} e_2^4 + \theta_1 \frac{1}{2} \lambda_1^2 + c_4^2 \frac{1}{2} \lambda_2^2 + 3c_4^2 \frac{1}{2} \lambda_3^2, \quad (26)$$

where W_1 is represented as

$$W_1 = \theta_1 \frac{1}{2\lambda_1^2} e_1^3 x_1^4 + \theta_3 x_1 + c_4^2 \frac{1}{2\lambda_2^2} e_1^3 \left(h(x_1) \frac{\partial h(x_1)}{\partial x_1} \right)^2 + \theta_4 \frac{3}{4} e_1 + 3c_4^2 \frac{1}{2\lambda_3^2} e_1 h^4(x_1). \quad (27)$$

The virtual control unit x_2^* in (26) is developed as

$$x_2^* = \mathcal{I}_{st}(\kappa_1) \bar{\alpha}_1, \quad (28)$$

where the adaptive law for κ_1 is given in (30), and $\bar{\alpha}_1$ is the designed equivalent virtual unit that is constructed as

$$\bar{\alpha}_1 = -k_1 e_1 - \left(\hat{\theta}_1 \frac{1}{2\lambda_1^2} e_1^3 x_1^4 + \hat{\theta}_3 x_1 + c_4^2 \frac{1}{2\lambda_2^2} e_1^3 \left(h(x_1) \frac{\partial h(x_1)}{\partial x_1} \right)^2 + \hat{\theta}_4 \frac{3}{4} e_1 + 3c_4^2 \frac{1}{2\lambda_3^2} e_1 h^4(x_1) \right), \tag{29}$$

where k_1 is the positive designed controller gain and $\hat{\theta}_1, \hat{\theta}_3, \hat{\theta}_4$, respectively, stand for the estimate of $\theta_1, \theta_3, \theta_4$. The adaptive law for (28) is constructed as

$$\dot{\kappa}_1 = -R_1 e_1^3 \bar{\alpha}_1, \tag{30}$$

where R_1 is a positive designed constant.

Consider the results in (26)–(30) and define the estimation error $\tilde{\theta}_1 = \theta_1 - \hat{\theta}_1$, $\tilde{\theta}_3 = \theta_3 - \hat{\theta}_3$, $\tilde{\theta}_4 = \theta_4 - \hat{\theta}_4$. Inequality (26) is thus rewritten as follows:

$$\begin{aligned} \mathcal{L}V_1 \leq & -(k_1 + \theta_2) e_1^4 - \theta_4 \mathcal{I}_{st}(\kappa_1) \frac{\dot{\kappa}_1}{R_1} + \frac{\dot{\kappa}_1}{R_1} + \theta_4 \frac{1}{4} e_2^4 + \theta_1 \frac{1}{2} \lambda_1^2 + c_4^2 \frac{1}{2} \lambda_2^2 + 3c_4^2 \frac{1}{2} \lambda_3^2 \\ & + \tilde{\theta}_1 \frac{1}{2\lambda_1^2} e_1^6 x_1^4 + \tilde{\theta}_3 e_1^4 + \tilde{\theta}_4 \frac{3}{4} e_1^4. \end{aligned} \tag{31}$$

Step 2: Augment the stochastic Lyapunov function of Step 2 as $V_2 = V_1 + \frac{1}{4} e_2^4$. The error dynamical equation of the second subsystem of the system (23) can be described as

$$\begin{aligned} de_2 &= dx_2 - dx_2^*, \\ &= (-\theta_5 x_2 + \theta_6 x_1 + c_3 x_1 + u - \mathcal{L}x_2^*) dt + \left(-\frac{\partial x_2^*}{\partial x_1} \sqrt{2} c_4 h(x_1) \right) dw, \end{aligned} \tag{32}$$

where we design the new control $u = f(x_1)x_3 + \theta_7 u_1$ to replace actual control u_1 .

The differential operator of x_2^* can be calculated using (16) as follows:

$$\begin{aligned} \mathcal{L}x_2^* &= -\theta_1 \frac{\partial x_2^*}{\partial x_1} x_1^2 - \theta_2 \frac{\partial x_2^*}{\partial x_1} x_1 + \theta_3 \frac{\partial x_2^*}{\partial x_1} x_1 + c_4^2 \frac{\partial x_2^*}{\partial x_1} h(x_1) \frac{\partial h(x_1)}{\partial x_1} + \theta_4 \frac{\partial x_2^*}{\partial x_1} x_2 + c_4^2 \frac{\partial^2 x_2^*}{\partial x_1^2} h^2(x_1) \\ &+ \frac{\partial x_2^*}{\partial \theta_1} \dot{\hat{\theta}}_1 + \frac{\partial x_2^*}{\partial \theta_3} \dot{\hat{\theta}}_3 + \frac{\partial x_2^*}{\partial \theta_4} \dot{\hat{\theta}}_4 + \frac{\partial x_2^*}{\partial \kappa_1} \dot{\kappa}_1. \end{aligned} \tag{33}$$

Recalling (16), (32) and (33), $\mathcal{L}V_2$ is presented as

$$\mathcal{L}V_2 = \mathcal{L}V_1 + e_2^3 (-\theta_5 x_2 + \theta_6 x_1 + c_3 x_1 + u - \mathcal{L}x_2^*) + 3c_4^2 e_2^2 \left(\frac{\partial x_2^*}{\partial x_1} h(x_1) \right)^2. \tag{34}$$

Employing Young’s inequality (19), one obtains that the term in (34) can be further changed into

$$3c_4^2 e_2^2 \left(\frac{\partial x_2^*}{\partial x_1} h(x_1) \right)^2 \leq 3c_4^2 \frac{1}{2\lambda_4^2} e_2^4 \left(\frac{\partial x_2^*}{\partial x_1} h(x_1) \right)^4 + 3c_4^2 \frac{1}{2} \lambda_4^2, \tag{35}$$

where the designed constant λ_4 is positive. Combining the results (31), (33)–(35), one can obtain inequality $\mathcal{L}V_2$ as follows:

$$\begin{aligned} \mathcal{L}V_2 \leq & -(k_1 + \theta_2) e_1^4 - \theta_4 \mathcal{I}_{st}(\kappa_1) \frac{\dot{\kappa}_1}{R_1} + \frac{\dot{\kappa}_1}{R_1} + e_2^3 (u + W_2) \\ & + \theta_1 \frac{1}{2} \lambda_1^2 + c_4^2 \frac{1}{2} \lambda_2^2 + 3c_4^2 \frac{1}{2} \lambda_3^2 + 3c_4^2 \frac{1}{2} \lambda_4^2 + \tilde{\theta}_1 \frac{1}{2\lambda_1^2} e_1^6 x_1^4 + \tilde{\theta}_3 e_1^4 + \tilde{\theta}_4 \frac{3}{4} e_1^4, \end{aligned} \tag{36}$$

where W_2 is defined as

$$\begin{aligned}
W_2 = & \theta_1 \frac{\partial x_2^*}{\partial x_1} x_1^2 + \theta_2 \frac{\partial x_2^*}{\partial x_1} x_1 - \theta_3 \frac{\partial x_2^*}{\partial x_1} x_1 + \theta_4 \frac{1}{4} e_2 - \theta_4 \frac{\partial x_2^*}{\partial x_1} x_2 - \theta_5 x_2 + \theta_6 x_1 + c_3 x_1 \\
& + 3c_4^2 \frac{1}{2\lambda_4^2} e_2 \left(\frac{\partial x_2^*}{\partial x_1} h(x_1) \right)^4 - c_4^2 \frac{\partial x_2^*}{\partial x_1} h(x_1) \frac{\partial h(x_1)}{\partial x_1} - c_4^2 \frac{\partial^2 x_2^*}{\partial x_1^2} h^2(x_1) \\
& - \frac{\partial x_2^*}{\partial \kappa_1} \dot{\kappa}_1 - \frac{\partial x_2^*}{\partial \theta_1} \dot{\theta}_1 - \frac{\partial x_2^*}{\partial \theta_3} \dot{\theta}_3 - \frac{\partial x_2^*}{\partial \theta_4} \dot{\theta}_4.
\end{aligned} \tag{37}$$

Then, we zoom $e_2^3 W_2$ to its upper bound as follows:

$$\begin{aligned}
e_2^3 W_2 \leq & \theta_1 \left| \frac{\partial x_2^*}{\partial x_1} e_2^3 x_1^2 \right| + \theta_2 \left| \frac{\partial x_2^*}{\partial x_1} e_2^3 x_1 \right| + \theta_3 \left| \frac{\partial x_2^*}{\partial x_1} e_2^3 x_1 \right| + \theta_4 \left| \frac{\partial x_2^*}{\partial x_1} e_2^3 x_2 \right| + \theta_5 \left| e_2^3 x_2 \right| + \theta_6 \left| e_2^3 x_1 \right| \\
& + \left| e_2^3 \left[c_3 x_1 - c_4^2 \frac{\partial x_2^*}{\partial x_1} h(x_1) \frac{\partial h(x_1)}{\partial x_1} - c_4^2 \frac{\partial^2 x_2^*}{\partial x_1^2} h^2(x_1) - \frac{\partial x_2^*}{\partial \kappa_1} \dot{\kappa}_1 - \frac{\partial x_2^*}{\partial \theta_1} \dot{\theta}_1 - \frac{\partial x_2^*}{\partial \theta_3} \dot{\theta}_3 - \frac{\partial x_2^*}{\partial \theta_4} \dot{\theta}_4 \right] \right| \\
& + \theta_4 \frac{1}{4} e_2^4 + 3c_4^2 \frac{1}{2\lambda_4^2} e_2^4 \left(\frac{\partial x_2^*}{\partial x_1} h(x_1) \right)^4.
\end{aligned} \tag{38}$$

According to Lemma 1, we design control signal u , and adaptive law κ_2 , equivalent virtual unit \bar{a}_2 as

$$u = \mathcal{I}_{st}(\kappa_2) \bar{a}_2, \tag{39}$$

$$\dot{\kappa}_2 = -R_2 e_2^3 \bar{a}_2, \tag{40}$$

$$\begin{aligned}
\bar{a}_2 = & -k_2 e_2 - \text{sgn}(e_2^3) \left(\hat{\theta}_1 \left| \frac{\partial x_2^*}{\partial x_1} x_1^2 \right| + \hat{\theta}_2 \left| \frac{\partial x_2^*}{\partial x_1} x_1 \right| + \hat{\theta}_3 \left| \frac{\partial x_2^*}{\partial x_1} x_1 \right| + \hat{\theta}_4 \left| \frac{\partial x_2^*}{\partial x_1} x_2 \right| + \hat{\theta}_5 |x_2| + \hat{\theta}_6 |x_1| \right. \\
& \left. + \left| c_3 x_1 - c_4^2 \frac{\partial x_2^*}{\partial x_1} h(x_1) \frac{\partial h(x_1)}{\partial x_1} - c_4^2 \frac{\partial^2 x_2^*}{\partial x_1^2} h^2(x_1) - \frac{\partial x_2^*}{\partial \kappa_1} \dot{\kappa}_1 - \frac{\partial x_2^*}{\partial \theta_1} \dot{\theta}_1 - \frac{\partial x_2^*}{\partial \theta_3} \dot{\theta}_3 - \frac{\partial x_2^*}{\partial \theta_4} \dot{\theta}_4 \right| \right) \\
& - \hat{\theta}_4 \frac{1}{4} e_2 - 3c_4^2 \frac{1}{2\lambda_4^2} e_2 \left(\frac{\partial x_2^*}{\partial x_1} h(x_1) \right)^4,
\end{aligned} \tag{41}$$

where $k_2 > 0$, $\hat{\theta}_2, \hat{\theta}_5, \hat{\theta}_6$ are estimates of $\theta_2, \theta_5, \theta_6$. Define the estimation error $\tilde{\theta}_2 = \theta_2 - \hat{\theta}_2$, $\tilde{\theta}_5 = \theta_5 - \hat{\theta}_5$, $\tilde{\theta}_6 = \theta_6 - \hat{\theta}_6$. The sign function in (41) is defined as

$$\text{sgn}(e_2^3) = \begin{cases} 1, & e_2^3 > 0 \\ 0, & e_2^3 = 0 \\ -1, & e_2^3 < 0. \end{cases} \tag{42}$$

In succession, the actual controller u_{rd} in (2) is presented as

$$u_{rq} = \frac{u - f(x_1)x_3}{\theta_7} + u_{rq}^*. \tag{43}$$

Considering the results in (37)–(41), (36) is thus presented as follows:

$$\begin{aligned}
\mathcal{L}V_2 \leq & -(k_1 + \vartheta_2) e_1^4 - k_2 e_2^4 - \theta_4 \mathcal{I}_{st}(\kappa_1) \frac{\dot{\kappa}_1}{R_1} + \frac{\dot{\kappa}_1}{R_1} - \mathcal{I}_{st}(\kappa_2) \frac{\dot{\kappa}_2}{R_2} + \frac{\dot{\kappa}_2}{R_2} + \theta_1 \frac{1}{2} \lambda_1^2 + c_4^2 \frac{1}{2} \lambda_2^2 \\
& + 3c_4^2 \frac{1}{2} \lambda_3^2 + 3c_4^2 \frac{1}{2} \lambda_4^2 + \tilde{\theta}_1 \left(\left| \frac{\partial x_2^*}{\partial x_1} e_2^3 x_1^2 \right| + \frac{1}{2\lambda_1^2} e_1^6 x_1^4 \right) + \tilde{\theta}_2 \left| \frac{\partial x_2^*}{\partial x_1} e_2^3 x_1 \right| + \tilde{\theta}_3 \left(\left| \frac{\partial x_2^*}{\partial x_1} e_2^3 x_1 \right| + e_1^4 \right) \\
& + \tilde{\theta}_4 \left(\left| \frac{\partial x_2^*}{\partial x_1} e_2^3 x_2 \right| + \frac{3}{4} e_1^4 + \frac{1}{4} e_2^4 \right) + \tilde{\theta}_5 |e_2^3 x_2| + \tilde{\theta}_6 |e_2^3 x_1|.
\end{aligned} \tag{44}$$

Step 3: Augment the stochastic Lyapunov function of Step 2 as $V_3 = V_2 + \frac{1}{4}e_3^4$. Notice that

$$\begin{aligned} de_3 &= dx_3 - dx_3^*, \\ &= (-\theta_5 x_3 - c_2 x_1 + c_1 x_2 - x_1 x_2 + \theta_7 u_2) dt. \end{aligned} \quad (45)$$

Considering the result of (44), the differential operator of $\mathcal{L}V_3$ is

$$\begin{aligned} \mathcal{L}V_3 &\leq -(k_1 + \theta_2)e_1^4 - k_2 e_2^4 - \theta_4 \mathcal{I}_{st}(\kappa_1) \frac{\dot{\kappa}_1}{R_1} + \frac{\dot{\kappa}_1}{R_1} - \mathcal{I}_{st}(\kappa_2) \frac{\dot{\kappa}_2}{R_2} + \frac{\dot{\kappa}_2}{R_2} - \theta_5 e_3^4 \\ &\quad + e_3^3 (W_3 + \theta_7 u_2) + \theta_1 \frac{1}{2} \lambda_1^2 + c_4^2 \frac{1}{2} \lambda_2^2 + 3c_4^2 \frac{1}{2} \lambda_3^2 + 3c_4^2 \frac{1}{2} \lambda_4^2 \\ &\quad + \tilde{\theta}_1 \left(\left| \frac{\partial x_2^*}{\partial x_1} e_2^3 x_1^2 \right| + \frac{1}{2\lambda_1^2} e_1^6 x_1^4 \right) + \tilde{\theta}_2 \left| \frac{\partial x_2^*}{\partial x_1} e_2^3 x_1 \right| + \tilde{\theta}_3 \left(\left| \frac{\partial x_2^*}{\partial x_1} e_2^3 x_1 \right| + e_1^4 \right) \\ &\quad + \tilde{\theta}_4 \left(\left| \frac{\partial x_2^*}{\partial x_1} e_2^3 x_2 \right| + \frac{3}{4} e_1^4 + \frac{1}{4} e_2^4 \right) + \tilde{\theta}_5 |e_2^3 x_2| + \tilde{\theta}_6 |e_2^3 x_1|, \end{aligned} \quad (46)$$

where $W_3 = -c_2 x_1 + c_1 x_2 - x_1 x_2$; then, one can obtain that

$$e_3^3 W_3 \leq |e_3^3| |-c_2 x_1 + c_1 x_2 - x_1 x_2|. \quad (47)$$

The control signal u_2 , equivalent virtual control \bar{a}_3 and adaptive law κ_3 are chosen as

$$u_2 = \mathcal{I}_{st}(\kappa_3) \bar{a}_3, \quad (48)$$

$$\bar{a}_3 = -k_3 e_3 - \text{sgn}(e_3^3) |-c_2 x_1 + c_1 x_2 - x_1 x_2|, \quad (49)$$

$$\dot{\kappa}_3 = -R_3 e_3^3 \bar{u}_2. \quad (50)$$

Subsequently, the actual controller u_{rd} is designed as

$$u_{rd} = \mathcal{I}_{st}(\kappa_3) \bar{a}_3 + u_{rd}^* \quad (51)$$

Thus, inequality (46) is transformed as

$$\begin{aligned} \mathcal{L}V_3 &\leq -(k_1 + \theta_2)e_1^4 - k_2 e_2^4 - (k_3 + \theta_5)e_3^4 - \theta_4 \mathcal{I}_{st}(\kappa_1) \frac{\dot{\kappa}_1}{R_1} + \frac{\dot{\kappa}_1}{R_1} - \mathcal{I}_{st}(\kappa_2) \frac{\dot{\kappa}_2}{R_2} + \frac{\dot{\kappa}_2}{R_2} \\ &\quad - \theta_7 \mathcal{I}_{st}(\kappa_3) \frac{\dot{\kappa}_3}{R_3} + \frac{\dot{\kappa}_3}{R_3} + \theta_1 \frac{1}{2} \lambda_1^2 + c_4^2 \frac{1}{2} \lambda_2^2 + 3c_4^2 \frac{1}{2} \lambda_3^2 + 3c_4^2 \frac{1}{2} \lambda_4^2 \\ &\quad + \tilde{\theta}_1 \left(\left| \frac{\partial x_2^*}{\partial x_1} e_2^3 x_1^2 \right| + \frac{1}{2\lambda_1^2} e_1^6 x_1^4 \right) + \tilde{\theta}_2 \left| \frac{\partial x_2^*}{\partial x_1} e_2^3 x_1 \right| + \tilde{\theta}_3 \left(\left| \frac{\partial x_2^*}{\partial x_1} e_2^3 x_1 \right| + e_1^4 \right) \\ &\quad + \tilde{\theta}_4 \left(\left| \frac{\partial x_2^*}{\partial x_1} e_2^3 x_2 \right| + \frac{3}{4} e_1^4 + \frac{1}{4} e_2^4 \right) + \tilde{\theta}_5 |e_2^3 x_2| + \tilde{\theta}_6 |e_2^3 x_1|. \end{aligned} \quad (52)$$

Step 4 : For the whole system (23), choose stochastic Lyapunov function $V = V_3 + \frac{1}{2\rho_1} \tilde{\theta}_1^2 + \frac{1}{2\rho_2} \tilde{\theta}_2^2 + \frac{1}{2\rho_3} \tilde{\theta}_3^2 + \frac{1}{2\rho_4} \tilde{\theta}_4^2 + \frac{1}{2\rho_5} \tilde{\theta}_5^2 + \frac{1}{2\rho_6} \tilde{\theta}_6^2$. $\rho_1 \sim \rho_6, \iota_1 \sim \iota_6$ are positive constants.

The parameter updating laws are designed for $\hat{\theta}_1, \hat{\theta}_2, \hat{\theta}_3, \hat{\theta}_4, \hat{\theta}_5, \hat{\theta}_6$ as follows:

$$\begin{aligned}
 \dot{\hat{\theta}}_1 &= \rho_1 \left(\left| \frac{\partial x_2^*}{\partial x_1} e_2^3 x_1^2 \right| + \frac{1}{2\lambda_1^2} e_1^6 x_1^4 \right) - \iota_1 \hat{\theta}_1 \\
 \dot{\hat{\theta}}_2 &= \rho_2 \left| \frac{\partial x_2^*}{\partial x_1} e_2^3 x_1 \right| - \iota_2 \hat{\theta}_2 \\
 \dot{\hat{\theta}}_3 &= \rho_3 \left(\left| \frac{\partial x_2^*}{\partial x_1} e_2^3 x_1 \right| + e_1^4 \right) - \iota_3 \hat{\theta}_3 \\
 \dot{\hat{\theta}}_4 &= \rho_4 \left(\left| \frac{\partial x_2^*}{\partial x_1} e_2^3 x_2 \right| + \frac{3}{4} e_1^4 + \frac{1}{4} e_2^4 \right) - \iota_4 \hat{\theta}_4 \\
 \dot{\hat{\theta}}_5 &= \rho_5 \left| e_2^3 x_2 \right| - \iota_5 \hat{\theta}_5 \\
 \dot{\hat{\theta}}_6 &= \rho_6 \left| e_2^3 x_1 \right| - \iota_6 \hat{\theta}_6.
 \end{aligned} \tag{53}$$

Based on (52) and (53), the differential operator of V is presented as

$$\begin{aligned}
 \mathcal{L}V &\leq -(k_1 + \theta_2)e_1^4 - k_2e_2^4 - (k_3 + \theta_5)e_3^4 \\
 &+ \frac{\rho_1}{\iota_1} \tilde{\theta}_1 \hat{\theta}_1 + \frac{\rho_2}{\iota_2} \tilde{\theta}_2 \hat{\theta}_2 + \frac{\rho_3}{\iota_3} \tilde{\theta}_3 \hat{\theta}_3 + \frac{\rho_4}{\iota_4} \tilde{\theta}_4 \hat{\theta}_4 + \frac{\rho_5}{\iota_5} \tilde{\theta}_5 \hat{\theta}_5 + \frac{\rho_6}{\iota_6} \tilde{\theta}_6 \hat{\theta}_6 \\
 &- \theta_4 \mathcal{I}_{st}(\kappa_1) \frac{\dot{\kappa}_1}{R_1} + \frac{\dot{\kappa}_1}{R_1} - \mathcal{I}_{st}(\kappa_2) \frac{\dot{\kappa}_2}{R_2} + \frac{\dot{\kappa}_2}{R_2} - \theta_7 \mathcal{I}_{st}(\kappa_3) \frac{\dot{\kappa}_3}{R_3} + \frac{\dot{\kappa}_3}{R_3} \\
 &+ \theta_1 \frac{1}{2} \lambda_1^2 + c_4^2 \frac{1}{2} \lambda_2^2 + 3c_4^2 \frac{1}{2} \lambda_3^2 + 3c_4^2 \frac{1}{2} \lambda_4^2.
 \end{aligned} \tag{54}$$

Employing Young’s inequality to $\frac{\rho_i}{\iota_i} \tilde{\theta}_i \hat{\theta}_i$, one can obtain

$$\frac{\rho_i}{\iota_i} \tilde{\theta}_i \hat{\theta}_i \leq -\frac{\rho_i}{2\iota_i} \tilde{\theta}_i^2 + \frac{\rho_i}{2\iota_i} \theta_i^2. \tag{55}$$

Substituting (55) into (54) yields

$$\begin{aligned}
 \mathcal{L}V &\leq -(k_1 + \theta_2)e_1^4 - k_2e_2^4 - (k_3 + \theta_5)e_3^4 \\
 &- \frac{\iota_1}{2\rho_1} \tilde{\theta}_1^2 - \frac{\iota_2}{2\rho_2} \tilde{\theta}_2^2 - \frac{\iota_3}{2\rho_3} \tilde{\theta}_3^2 - \frac{\iota_4}{2\rho_4} \tilde{\theta}_4^2 - \frac{\iota_5}{2\rho_5} \tilde{\theta}_5^2 - \frac{\iota_6}{2\rho_6} \tilde{\theta}_6^2 \\
 &- \theta_4 \mathcal{I}_{st}(\kappa_1) \frac{\dot{\kappa}_1}{R_1} + \frac{\dot{\kappa}_1}{R_1} - \mathcal{I}_{st}(\kappa_2) \frac{\dot{\kappa}_2}{R_2} + \frac{\dot{\kappa}_2}{R_2} - \theta_7 \mathcal{I}_{st}(\kappa_3) \frac{\dot{\kappa}_3}{R_3} + \frac{\dot{\kappa}_3}{R_3} \\
 &+ \theta_1 \frac{1}{2} \lambda_1^2 + c_4^2 \frac{1}{2} \lambda_2^2 + 3c_4^2 \frac{1}{2} \lambda_3^2 + 3c_4^2 \frac{1}{2} \lambda_4^2 \\
 &+ \frac{\iota_1}{2\rho_1} \theta_1^2 + \frac{\iota_2}{2\rho_2} \theta_2^2 + \frac{\iota_3}{2\rho_3} \theta_3^2 + \frac{\iota_4}{2\rho_4} \theta_4^2 + \frac{\iota_5}{2\rho_5} \theta_5^2 + \frac{\iota_6}{2\rho_6} \theta_6^2.
 \end{aligned} \tag{56}$$

Asymptotic Stability Analysis

The nonlinear stochastic adaptive control for DFIG-WT is designed completely. Given that the stochastic system (23), the adaptive laws (30), (40), (50) and (53), the virtual control x_2^* (28) in step 1, the designed controllers u_{rq}, u_{rd} of DFIG-WT, respectively, in (43) and (51) are constructed, one draws the following conclusions:

1. State error variables e_1, e_2, e_3 , parameter error variables $\tilde{\theta}_1 \sim \tilde{\theta}_6$ and the adaptive laws $\kappa_1, \kappa_2, \kappa_3$ are kept bounded in probability.
2. ω_r asymptotically converges to ω_r^* in probability.

One can deduce the above-mentioned conclusions by Lemmas 1 and 3 as follows:

Step 1: From the observation of (56), the stochastic Lyapunov function of system (23) can be rewritten as

$$\mathcal{L}V \leq -\rho V(t) - \theta_4 \mathcal{I}_{st}(\kappa_1) \frac{\dot{\kappa}_1}{R_1} + \frac{\dot{\kappa}_1}{R_1} - \mathcal{I}_{st}(\kappa_2) \frac{\dot{\kappa}_2}{R_2} + \frac{\dot{\kappa}_2}{R_2} - \theta_7 \mathcal{I}_{st}(\kappa_3) \frac{\dot{\kappa}_3}{R_3} + \frac{\dot{\kappa}_3}{R_3} + \chi, \quad (57)$$

where $\rho = \min\{4(k_1 + \theta_2), 4k_2, 4(k_3 + \theta_5), \iota_1, \iota_2, \iota_3, \iota_4, \iota_5, \iota_6\}$, and $\chi = \theta_1 \frac{1}{2} \lambda_1^2 + c_{4\frac{1}{2}}^2 \lambda_2^2 + 3c_{4\frac{1}{2}}^2 \lambda_3^2 + 3c_{4\frac{1}{2}}^2 \lambda_4^2 + \sum_{i=1}^6 \frac{\iota_i}{2\rho_i} \theta_i^2$. The result of boundness in Lemma 1 can be directly utilized for (57). By the analysis in [26], t can be further extended to $t = \infty$. Immediately, one obtains that state error variables e_1, e_2, e_3 , parameter error variables $\tilde{\theta}_1 \sim \tilde{\theta}_6$ and the adaptive laws $\kappa_1, \kappa_2, \kappa_3$ are bounded in probability.

Step 2: We set $\hat{\theta}_i(0) \geq 0$ for $i = 1, 2, \dots, 6$. See Lemma 1 in [16]. One thus obtains that $\hat{\theta}_i(t)$ in (53) are non-negative. Hence, from (29), (41) and (49), the following constraints must hold:

$$e_i^3 \bar{\alpha}_i \leq -k_i e_i^4, \quad i = 1, 2, 3. \quad (58)$$

Hence, the right of the adaptive laws (30), (40) and (50) is non-negative. According to (58), we have

$$\dot{\kappa}_i(t) \geq R_i k_i e_i^4, \quad i = 1, 2, 3, \quad (59)$$

where $\kappa_i(0)$, $i = 1, 2, 3$ are set as a bounded variable and the boundness of $\kappa_i(t)$, $i = 1, 2, 3$ is derived from (57). It is noted that $k_1, k_2, k_3, R_1, R_2, R_3$ in (59) are designed as bounded constants. In succession, taking the integration and seeking expectation of (59) yields

$$E \int_0^t k_i R_i e_i^4 < +\infty, \quad i = 1, 2, 3, \quad (60)$$

Subsequently, utilizing Lemma 3, one can obtain

$$P \left\{ \lim_{t \rightarrow \infty} |e_i(t)| = 0 \right\} = 1, \quad i = 1, 2, 3. \quad (61)$$

From (61) and the definition of e_1 , one concludes that the rotor speed ω_r asymptotically converges to its desired value ω_r^* in probability.

5. Simulation Results

The simulation was established in a Python program for a 660 kW machine. In all simulations, we used the parameters of the wind turbine [14] and generator [18], as shown in Table 1. The following operating point is chosen as: $\omega_r^* = 284$ rad/s, $i_{rd}^* = 0$ A, $i_{rq}^* = -85.3036$ A by letting the right of (1), (2) and (14) equal zero. The function $h(x)$ in (12) in this paper is chosen as $h(x) = k_0 x(x^2 + 1)$ [27] by means of modeling wind speed based on stochastic processes. And note that a, b, c are the coefficients of the quadratic polynomial fit for T_m at a stochastic wind speed whose mean value is 15 m/s.

In this section, a new stochastic asymptotic control is designed for the wind turbine with stochastic wind speed.

The initial conditions for the DFIG-WT system are designed as $[x_1(0), x_2(0), x_3(0)]^T = [-3, 0.1, 0.1]^T$, and initial conditions for adaptive laws $\kappa_i, \hat{\theta}_i$, $i = 1, 2, 3$ are all set to be zero. The controller parameters $k_1 \sim k_3, R_1 \sim R_3, \lambda_1 \sim \lambda_4, \rho_1 \sim \rho_6, \iota_1 \sim \iota_6$ of the stochastic backstepping control are chosen as follows: To avoid instability, $\rho_i > 0, i = 1, 2, \dots, 6$ must be satisfied, and to guarantee the adaptive rate of $\hat{\theta}_i, i = 1, 2, \dots, 6$, we choose $\rho_1 = 20, \rho_2 = 12, \rho_3 = 15, \rho_4 = 12, \rho_5 = 10$ and $\rho_6 = 6$. Furthermore, the adaptive rate of $\kappa_i, i = 1, 2, 3$ can be controlled by increasing R_1, R_2, R_3 . Hence, we select $R_1 = 10, R_2 = 1000$ and $R_3 = 10$ in this simulation. Similarly, $k_1 = 308, k_2 = 121$ and $k_3 = 100$ are chosen. The parameters $\iota_i, i = 1, 2, \dots, 6$ are chosen according to the work in [16] showing that smaller gain will improve convergence performance. In addition, large positive gain $\lambda_1 = 10, \lambda_2 = 10, \lambda_3 = 10, \lambda_4 = 10$ can be obtained to satisfy young's inequality of (19).

Table 1. Parameters in simulations.

Name	Symbol	Value	Unit
The length of blade	R	15	m
Rated stator voltage	V_s	380	V
Rated stator frequency	f	50	Hz
Number of pole pairs	pn	2	pu
Stator winding resistance	R_s	2.65	m Ω
Rotor winding resistance	R_r	2.63	m Ω
Stator winding inductance	L_s	5.6438	mH
Rotor winding inductance	L_r	5.6068	mH
Magnetizing inductance	L_m	5.4749	mH
Gearbox ratio	N	2	pu
Inertia of system	J	0.1	kg·m ²
Mean wind speed	\bar{V}_w	15	m/s
Fitting parameter 1	a	−0.002202	pu
Fitting parameter 2	b	1.272	pu
Fitting parameter 3	c	−83.55	pu
Optimal tip speed ratio	λ_{opt}	7.1	pu
Intensity of the white noise	K	1	pu
Gain of function $h(\omega_r - \omega_r^*)$	k_0	0.01	pu

The following two cases are considered to validate the effectiveness of the proposed controller.

Case 1: All physical parameters are known and kept constant;

Case 2: Values $a, b, c, L_s, L_r, L_m, R_r$ are unknown and subject to slow variation due to the complex operating conditions compared with the conventional backstepping method.

The simulation results presented in Figures 5–12 reveal the following findings:

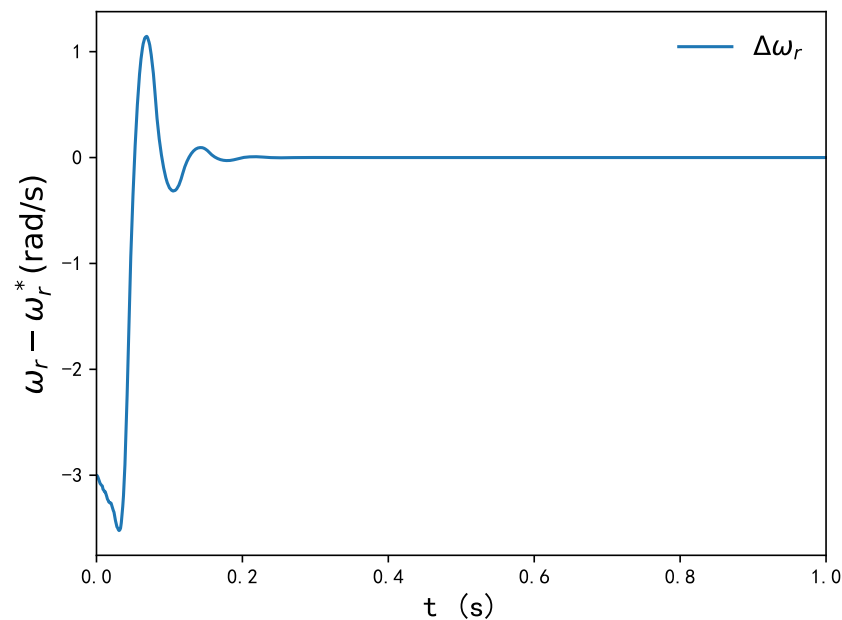


Figure 5. Error between rotor speed and its reference with no parameter estimate.

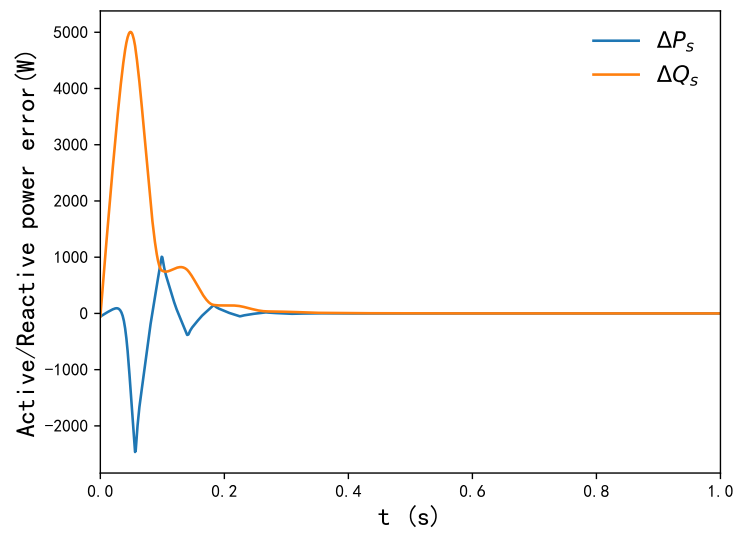


Figure 6. Errors between active/reactive power and their reference with no parameter estimate.

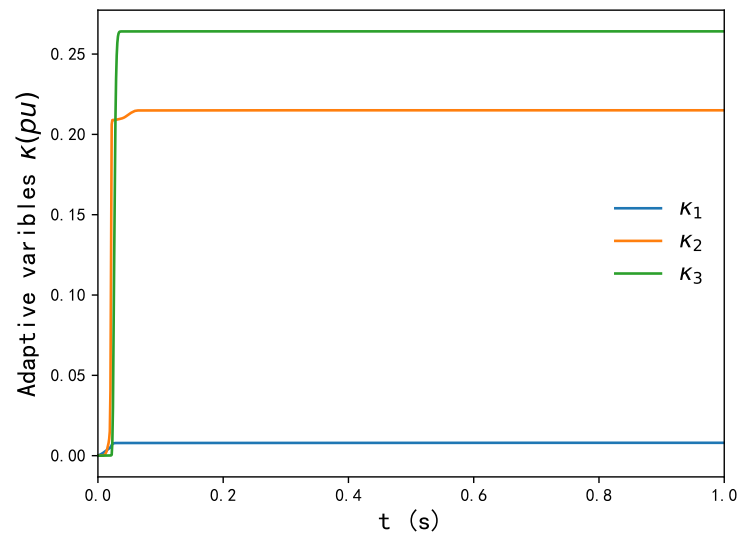


Figure 7. Adaptive statement with no parameter estimate.

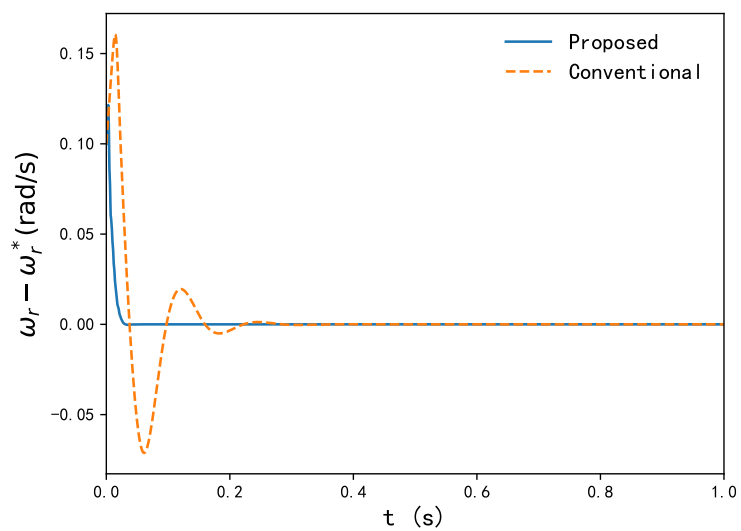


Figure 8. Error between rotor speed and its reference with parameter estimate.

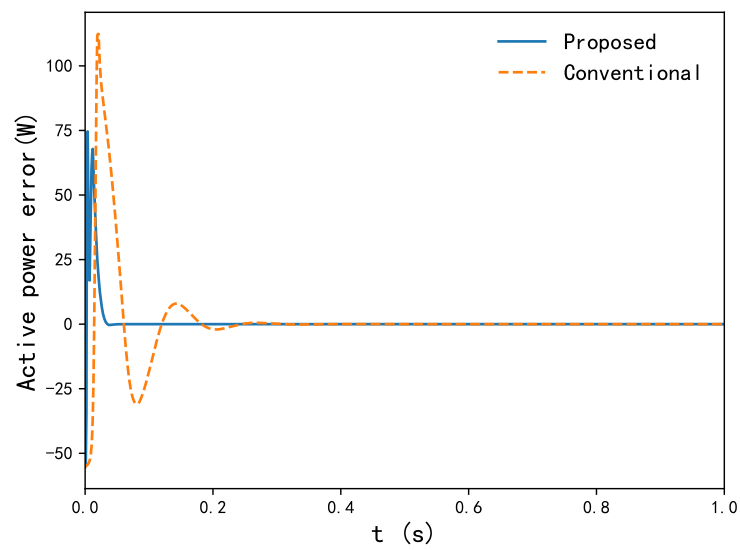


Figure 9. Active power error with parameter estimate.

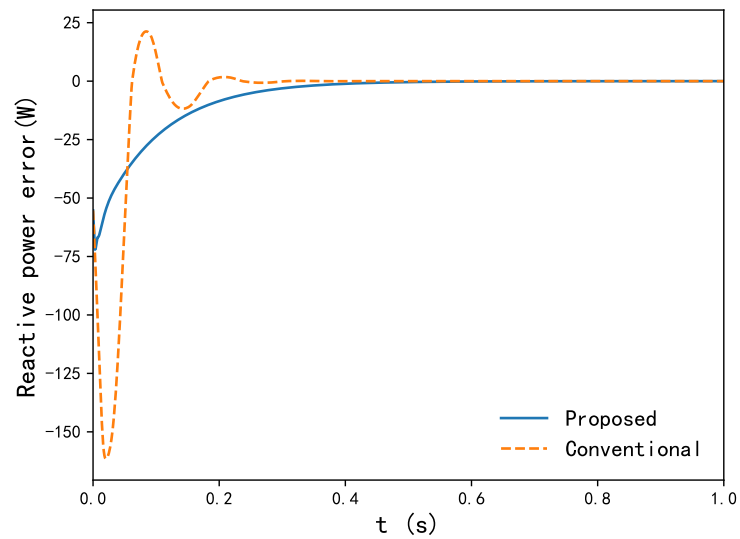


Figure 10. Reactive power error with parameter estimate.

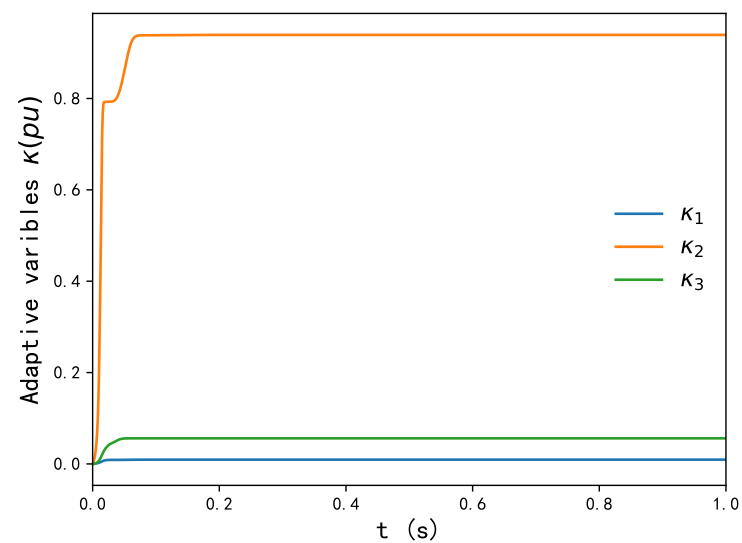


Figure 11. Adaptive statement with parameter estimate.

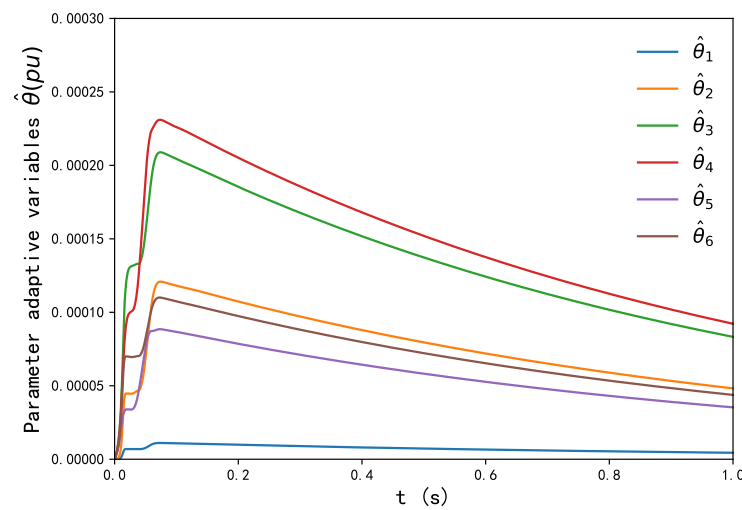


Figure 12. Parameter adaptive statement with parameter estimate.

(1) Concerning the output active/reactive power of DFIG-WT, Figure 6 depicts the error between power reference P_s^*, Q_s^* and P_s, Q_s . The figures show that when the wind velocity fluctuates the mean value with white noise up and down, the errors between P_s^*, Q_s^* and P_s, Q_s are approximately zero with the proposed method. This is mainly because the torque coefficient C_q remains around C_{qmax} , as shown in Figure 2. In other words, with the proposed method, the main objective, which is to have P_s, Q_s to P_s^*, Q_s^* , is completely achieved. Rotor speed ω_r converges swiftly to its optimal speed (9) at 2.2 s, as shown in Figure 5. In the meantime, adaptive laws κ_1, κ_2 and κ_3 for updating the virtual controller are presented in Figure 7. As depicted in Figure 7, adaptive laws containing κ_1, κ_2 and κ_3 quickly converge to stable values with the proposed controller. Therefore, it is shown that the proposed controller has the capacity of achieving the asymptotic control for stochastic nonlinear systems of DFIG-WT.

(2) In Case 2, the parameters of the system are subject to changes due to various physical phenomena; so, our controller should provide effective control when the variation of the generator parameters is bounded in comparison with the conventional backstepping controller. In order to test the robustness of the controller, we varied the rotor resistance R_r to $2R_r$, the inductance value of the rotor and stator 10% from its nominal value and the parameters a, b, c of mechanical torque 5% from their current value.

Similarly, Figures 8–10 demonstrate that in Case 2, $\Delta\omega_r, \Delta P_s$ and ΔQ_s converge to zero, while ω_r, P_s and Q_s converge to their desired references. With the conventional method, however, the convergence rate is much slower compared with proposed controller. Figure 12 shows $\hat{\theta}_i, i = 1, 2, \dots, 6$ are always positive if its initial values are non-negative. Again, adaptive laws containing κ_1, κ_2 and κ_3 converge to stability with the proposed controller in Figure 11. Figures 8–12 show the effectiveness of varying the parameters of the generator R_r, L_s and L_r on the response of ω_r, i_{rd} and i_{rq} , which is directly related to the output active power and reactive power of DFIG-WT, and the performance with variation of parameters is effective for its swift convergence to the desired trajectory compared with the conventional backstepping controller.

6. Conclusions

An Itô stochastic differential model for DFIG-WT is introduced. Then, a new nonlinear stochastic adaptive backstepping controller for DFIG-WT is designed for the boundness of rotor speed and rotor current in probability. Further, an inequality technique is employed to extend the bounded control result to the asymptotic control. The variation of parameters of DFIG-WT is investigated with the adaptive controller. Furthermore, with the proposed controller, the rotor speed can asymptotically converge to its desired value to extract maximum power from stochastic wind energy. From a conceptual point of view, we could notice that

the nonlinear stochastic adaptive backstepping control is simple and easy to implement for the parameters of controller that are set in a certain regulation with gain suppressing inequality compared with conventional PI controller. The main risk is that the proposed controller is designed so that all inclusive signals are bounded in probability. We employ the stochastic Barbalat lemma to achieve the asymptotic convergence in probability of the output active/reactive power of DFIG-WT. That means one may obtain unstable results in some probabilities. But one can guarantee that the rotor speed converges asymptotically to the reference value almost surely according to the stochastic Barbalat lemma.

Author Contributions: Conceptualization, J.Z. and Y.W.; methodology, J.Z.; software, J.Z., Y.W. and M.D.; validation, J.Z., Y.W. and Q.O.; formal analysis, Y.W. and Q.O.; investigation, J.Z.; writing—original draft preparation, J.Z.; writing—review and editing, J.Z., Y.W. and M.D.; project administration, Y.W. and Q.O.; funding acquisition, Y.W. All authors have read and agreed to the published version of the manuscript.

Funding: This research was funded by National Natural Science Foundation of China, under Grant 61403194 and Grant 62173180.

Data Availability Statement: Not applicable.

Conflicts of Interest: The authors declare no conflict of interest.

References

1. Zhi, D.; Xu, L. Direct Power Control of DFIG with Constant Switching Frequency and Improved Transient Performance. *IEEE Trans. Energy Convers.* **2007**, *22*, 110–118. [[CrossRef](#)]
2. Xu, L.; Cartwright, P. Direct active and reactive power control of DFIG for wind energy generation. *IEEE Trans. Energy Convers.* **2006**, *21*, 750–758. [[CrossRef](#)]
3. Gao, S.; Zhao, H.; Gui, Y.; Zhou, D.; Blaabjerg, F. An Improved Direct Power Control for Doubly Fed Induction Generator. *IEEE Trans. Power Electron.* **2021**, *36*, 4672–4685. [[CrossRef](#)]
4. Zhang, Y.; Jiao, J.; Xu, D. Direct Power Control of Doubly Fed Induction Generator Using Extended Power Theory under Unbalanced Network. *IEEE Trans. Power Electron.* **2019**, *34*, 12024–12037. [[CrossRef](#)]
5. Pan, C.T.; Juan, Y.L. A Novel Sensorless MPPT Controller for a High-Efficiency Microscale Wind Power Generation System. *IEEE Trans. Energy Convers.* **2010**, *25*, 207–216.
6. Xiong, L.; Li, P.; Li, H.; Wang, J. Sliding Mode Control of DFIG Wind Turbines with a Fast Exponential Reaching Law. *Energies* **2017**, *10*, 1788. [[CrossRef](#)]
7. Yang, X.; Liu, G.; Li, A.; Le, V.D. A Predictive Power Control Strategy for DFIGs Based on a Wind Energy Converter System. *Energies* **2017**, *10*, 1098. [[CrossRef](#)]
8. Zhang, Y.; Jiang, T. Robust Predictive Rotor Current Control of a Doubly Fed Induction Generator under an Unbalanced and Distorted Grid. *IEEE Trans. Energy Convers.* **2022**, *37*, 433–442. [[CrossRef](#)]
9. Fateh, F.; White, W.N.; Gruenbacher, D. A Maximum Power Tracking Technique for Grid-Connected DFIG-Based Wind Turbines. *IEEE J. Emerg. Sel. Top. Power Electron.* **2015**, *3*, 957–966. [[CrossRef](#)]
10. Zhang, X.; Zhang, Z.; Jia, J.; Zheng, L. A Maximum Power Point Tracking Control Method Based on Rotor Speed PDF Shape for Wind Turbines. *Appl. Sci.* **2022**, *12*, 9108. [[CrossRef](#)]
11. Dang, D.Q.; Wang, Y.; Cai, W. Offset-Free Predictive Control for Variable Speed Wind Turbines. *IEEE Trans. Sustain. Energy* **2013**, *4*, 2–10. [[CrossRef](#)]
12. Xiong, P.; Sun, D. Backstepping-Based DPC Strategy of a Wind Turbine-Driven DFIG under Normal and Harmonic Grid Voltage. *IEEE Trans. Power Electron.* **2016**, *31*, 4216–4225. [[CrossRef](#)]
13. Kammoun, S.; Sallem, S.; Kammoun, M.B.A. Backstepping Control for Low-Voltage Ride Through Enhancement of DFIG-Based Wind Turbines. *Arab. J. Sci. Eng.* **2017**, *42*, 5083–5099. [[CrossRef](#)]
14. Mechter, A.; Kemih, K.; Ghanes, M. Backstepping control of a wind turbine for low wind speeds. *Nonlinear Dyn.* **2016**, *84*, 2435–2445. [[CrossRef](#)]
15. Bossoufi, B.; Karim, M.; Lagrioui, A.; Taoussi, M.; Derouich, A. Observer backstepping control of DFIG-Generators for wind turbines variable-speed: FPGA-based implementation. *Renew. Energy* **2015**, *81*, 903–917.
16. Chen, C.; Liu, Z.; Zhang, Y.; Chen, C.L.P.; Xie, S. Asymptotic Fuzzy Tracking Control for a Class of Stochastic Strict-Feedback Systems. *IEEE Trans. Fuzzy Syst.* **2017**, *25*, 556–568. [[CrossRef](#)]
17. Beltran, B.; Benbouzid, M.E.H.; Ahmed-Ali, T. Second-Order Sliding Mode Control of a Doubly Fed Induction Generator Driven Wind Turbine. *IEEE Trans. Energy Convers.* **2012**, *27*, 261–269. [[CrossRef](#)]
18. Phan, D.C.; Yamamoto, S. Rotor Speed Control of Doubly Fed Induction Generator Wind Turbines Using Adaptive Maximum Power Point Tracking. *Energy* **2016**, *111*, 377–388. [[CrossRef](#)]

19. Hu, J.; Nian, H.; Hu, B.; He, Y.; Zhu, Z. Direct active and reactive power regulation of DFIG using sliding-mode control approach. *IEEE Trans. Energy Convers.* **2010**, *25*, 1028–1039. [[CrossRef](#)]
20. Yuan, B.; Zhou, M.; Li, G.; Zhang, X.P. Stochastic Small-Signal Stability of Power Systems with Wind Power Generation. *IEEE Trans. Power Syst.* **2015**, *30*, 1680–1689. [[CrossRef](#)]
21. Pidre, J.; Carrillo, C.; Lorenzo, A. Probabilistic model for mechanical power fluctuations in asynchronous wind parks. *IEEE Trans. Power Syst.* **2003**, *18*, 761–768. [[CrossRef](#)]
22. Milano, F.; Zárate-Miñano, R. A Systematic Method to Model Power Systems as Stochastic Differential Algebraic Equations. *IEEE Trans. Power Syst.* **2013**, *28*, 4537–4544. [[CrossRef](#)]
23. Lin, Y.K. *Probabilistic Theory of Structural Dynamics*; Krieger: Melbourne, FL, USA, 1976.
24. Hu, X.L. An extension of Young’s inequality and its application. *Appl. Math. Comput.* **2013**, *219*, 6393–6399. [[CrossRef](#)]
25. Yu, X.; Wu, Z. Corrections to “Stochastic Barbalat’s Lemma and Its Applications” [Jun 12 1537–1543]. *IEEE Trans. Autom. Control* **2014**, *59*, 1386–1390. [[CrossRef](#)]
26. Ding, Z. Adaptive consensus output regulation of a class of nonlinear systems with unknown high-frequency gain. *Automatica* **2015**, *51*, 348–355. [[CrossRef](#)]
27. Obukhov, S.; Ibrahim, A.; Davydov, D.Y.; Alharbi, T.; Ahmed, E.M.; Ali, Z.M. Modeling Wind Speed Based on Fractional Ornstein-Uhlenbeck Process. *Energies* **2021**, *14*, 5561. [[CrossRef](#)]

Disclaimer/Publisher’s Note: The statements, opinions and data contained in all publications are solely those of the individual author(s) and contributor(s) and not of MDPI and/or the editor(s). MDPI and/or the editor(s) disclaim responsibility for any injury to people or property resulting from any ideas, methods, instructions or products referred to in the content.